

University of Groningen

Improved coronary artery calcium (CAC) detection in conventional CT with deep-learning image de-blurring

Wülker, Christian; van der Werf, Niels R.; Schnellbacher, Nikolas D.; Greuter, Marcel J.W.; Grass, Michael

Published in:
Medical Imaging 2024

DOI:
[10.1117/12.3006693](https://doi.org/10.1117/12.3006693)

IMPORTANT NOTE: You are advised to consult the publisher's version (publisher's PDF) if you wish to cite from it. Please check the document version below.

Document Version
Publisher's PDF, also known as Version of record

Publication date:
2024

[Link to publication in University of Groningen/UMCG research database](#)

Citation for published version (APA):

Wülker, C., van der Werf, N. R., Schnellbacher, N. D., Greuter, M. J. W., & Grass, M. (2024). Improved coronary artery calcium (CAC) detection in conventional CT with deep-learning image de-blurring. In R. Fahrig, J. M. Sabol, & K. Li (Eds.), *Medical Imaging 2024: Physics of Medical Imaging* (Vol. 12925). Article 129252B (Progress in Biomedical Optics and Imaging - Proceedings of SPIE; Vol. 12925). SPIE. <https://doi.org/10.1117/12.3006693>

Copyright

Other than for strictly personal use, it is not permitted to download or to forward/distribute the text or part of it without the consent of the author(s) and/or copyright holder(s), unless the work is under an open content license (like Creative Commons).

The publication may also be distributed here under the terms of Article 25fa of the Dutch Copyright Act, indicated by the "Taverne" license. More information can be found on the University of Groningen website: <https://www.rug.nl/library/open-access/self-archiving-pure/taverne-amendment>.

Take-down policy

If you believe that this document breaches copyright please contact us providing details, and we will remove access to the work immediately and investigate your claim.

Downloaded from the University of Groningen/UMCG research database (Pure): <http://www.rug.nl/research/portal>. For technical reasons the number of authors shown on this cover page is limited to 10 maximum.

Improved coronary artery calcium (CAC) detection in conventional CT with deep-learning image de-blurring

Christian Wülker^a, Niels R. van der Werf^b, Nikolas D. Schnellbacher^a, Marcel J. W. Greuter^c, and Michael Grass^a

^a Philips Innovative Technologies, Hamburg, Germany, ^b Philips Healthcare, Eindhoven, The Netherlands

^c University Medical Center Groningen, The Netherlands



Abstract

We investigated the impact of a CNN-based deep-learning (DL) algorithm for image de-blurring on coronary artery calcium (CAC) detection performance in conventional CT imaging. Our approach comprises first de-noising the image with a state-of-the-art CNN-based image de-noising algorithm. With improved SNR, it is then possible to sharpen the image with a CNN-based image de-blurring algorithm. We train such networks using natural images, *i.e.*, a large set of diverse photographs. The de-noising strength in the final image can be adjusted by blending back the estimated noise from the first step to the desired degree. To assess the impact of the de-blurring algorithm, we scanned an anthropomorphic phantom containing 100 small calcifications on a CT system using a CAC scoring protocol. Data were acquired at clinical and high radiation dose, and subsequently reconstructed with and without the DL de-blurring algorithm, using 25% de-noising strength. For each small CAC, detectability was defined as the ability to calculate an Agatston score (at least 3 adjacent voxels exceeding 130 Hounsfield units). For the high dose scans, CAC detectability increased from 39% for the standard reconstruction to 49% with de-blurring. The same 39% CAC detectability at high dose without de-blurring was obtained with routine dose with de-blurring. In this work, we also show some visual impressions of applying our DL de-blurring method to clinical cardiac data.

Introduction

- CT imaging suffers both from **noise** and **system blur**, which both impair **readability**, general **image quality** and the **diagnostic value** of any CT acquisition.
- This is in particular relevant for all clinical tasks involving the detection of small objects, such as **coronary artery calcification (CAC) detection**.
- In this work we assess the impact of a deep-learning, **CNN-based de-blurring** solution which we use together with a **CNN-based denoising** algorithm [1, 6], on the performance of CAC detection.
- For the quantification we evaluate CAC detection on a one-of-a-kind **anthropomorphic phantom** [3, 4], containing many various small cylindrical CACs of different sizes and densities.
- Algorithmically we use a separate denoising CNN followed by a de-blurring CNN (**two-steps**), giving us more flexibility and control in the output definition as opposed to a single end-to-end algorithm.

Methods

- The anthropomorphic **chest phantom** was scanned on a Philips CT7500 dual-layer system with a central **insert containing 100 small cylindrical calcifications**.
- Calcifications are varying in **size** (0.5 - 2mm) and **density** (90 - 540mg hydroxyapatite per cc).

Data acquisition parameters

- 120 kVp, 0.27s rot. time, 128 x 0.625 mm coll.
- 512 x 512 FBP recon with Philips standard res. C-filter and 220m FOV
- two dose settings: **clinical** dose (4.0 mGy CTDIvol) and **high** dose (20.8 mGy CTDIvol)

Figure 1 Axial view of the used phantom with the different calcifications clearly visible in the central insert. Figure taken from Ref. [3].

DL - deblurring workflow

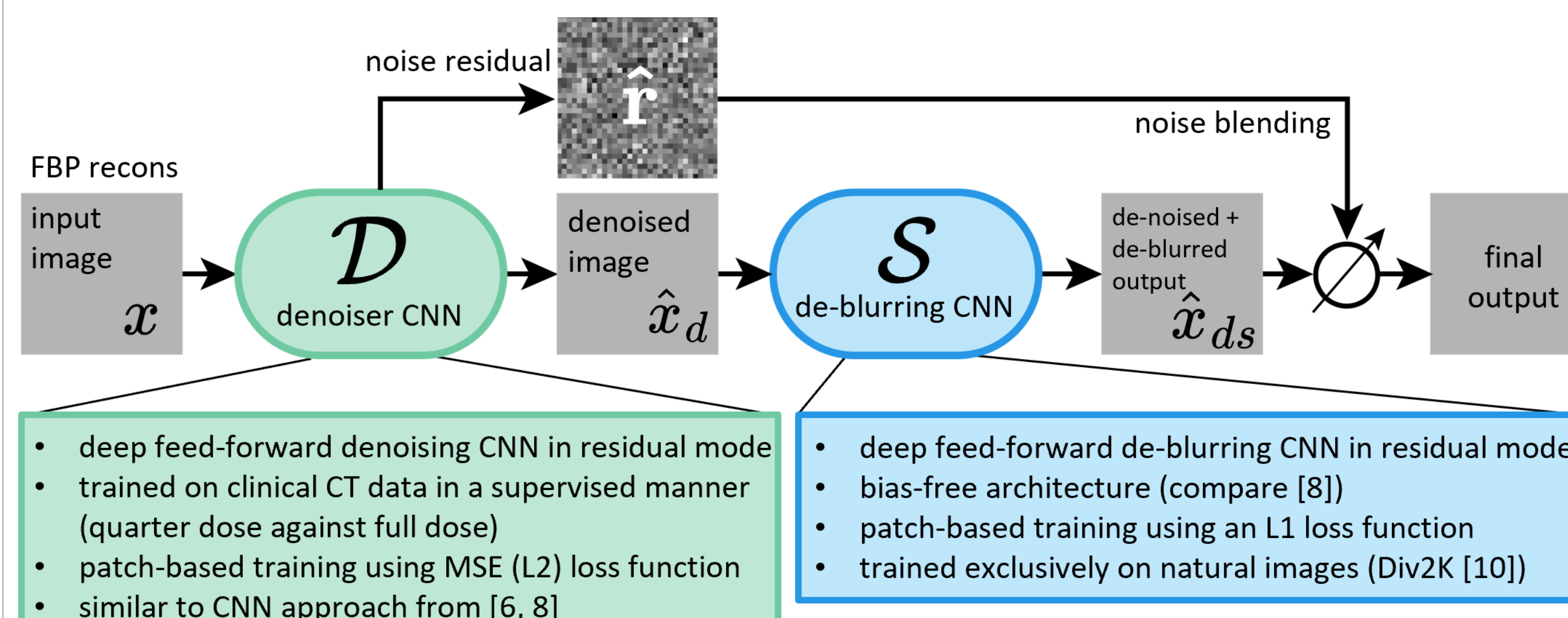


Figure 2 Schematic depiction of the introduced AI-deblurring solution. Starting with conv. FBP CT recons, we feed the images first to a denoising CNN, giving us a denoised image and an estimate for the noise residual in the image. In a second step we apply the AI-deblurring CNN to remove system blur from the images. Final noise blending with the stored noise residuals allows to control the noise level in the final output image.

Results

- CAC performance was assessed using a previously validated, automated quantification method [11], where for each **CAC detectability** was defined as the ability to calculate an Agatston score.

CAC detection accuracy

dose setting	standard	AI de-blurred
clinical	37 %	39 %
high	39 %	49 %

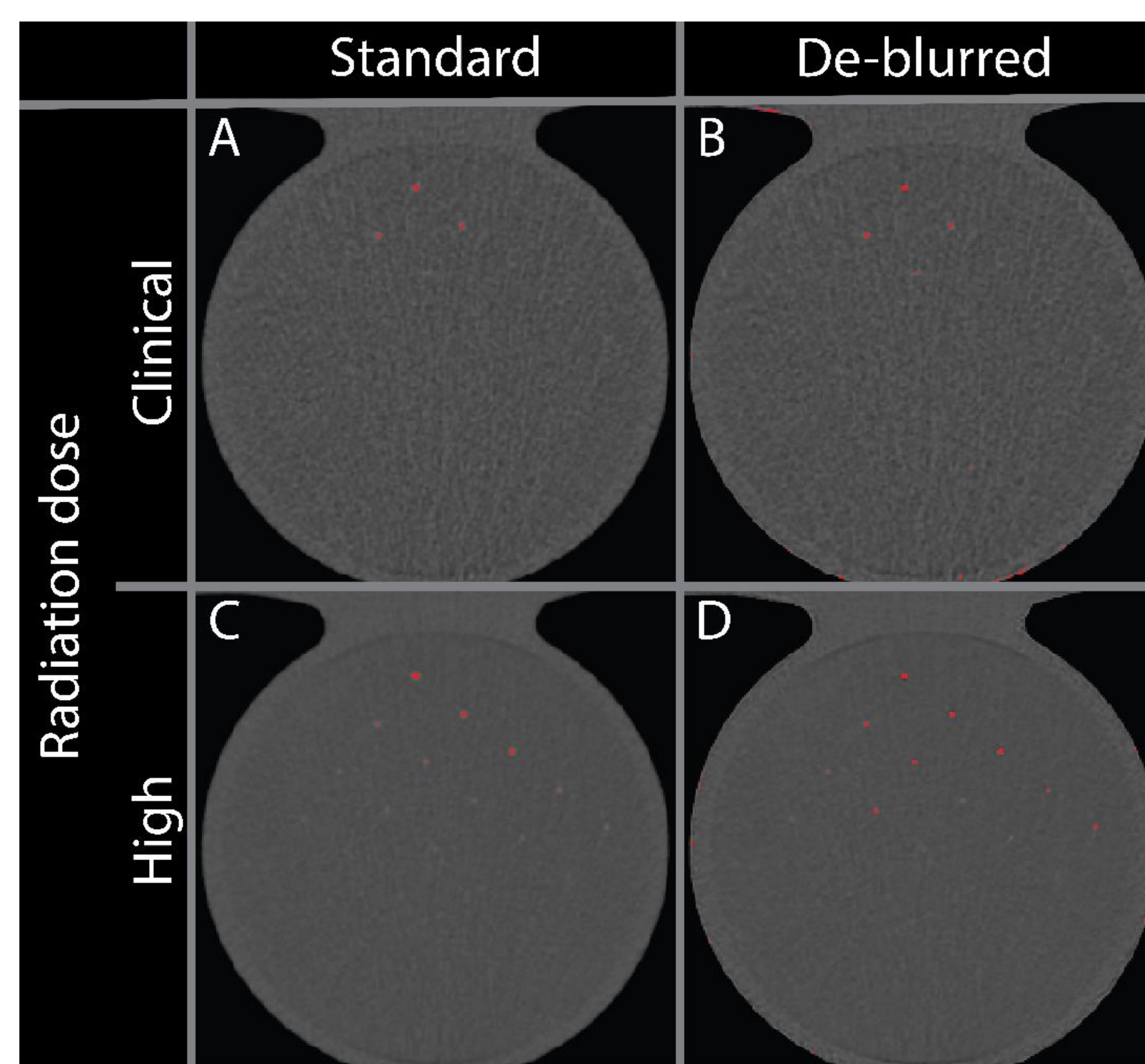


Figure 3 Representative images of the CAC phantom with voxels exceeding the Agatston scoring threshold of 130 HU labeled in red. The slice shown contains the 25 smallest (0.5 - 1.0 mm) and highest density (240 - 540 mg hydroxyapatite/cc) calcifications. Results are shown for (A) clinical dose and standard reconstruction, (B) clinical dose and DL de-blurred reconstruction, (C) high dose and standard reconstruction, and (D) high dose and DL de-blurred reconstruction. All images are shown at a level of 90 HU and window width of 750 HU.

Application to clinical cardiac CT

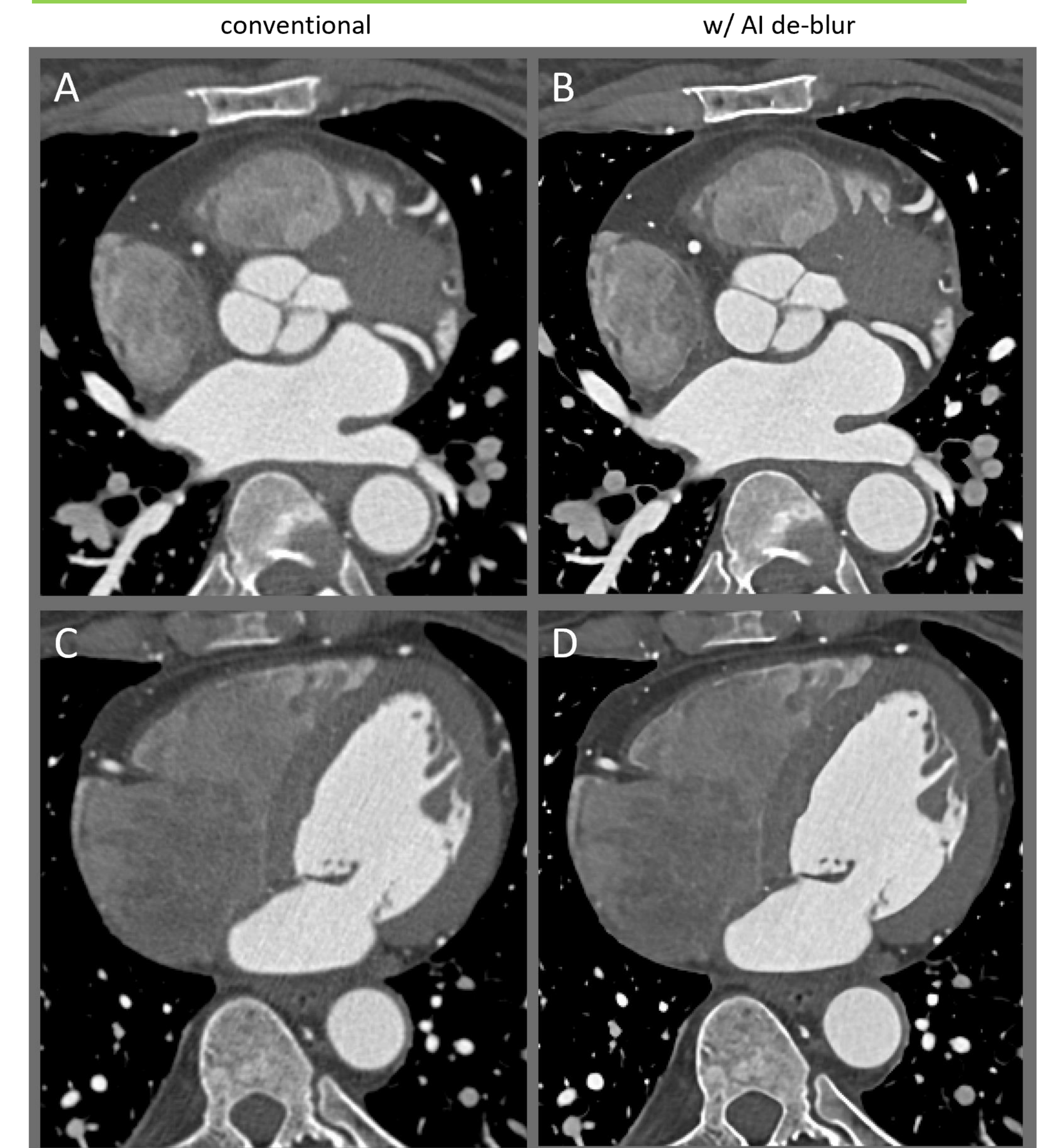


Figure 4 Gated cardiac CT acquisition shown at two different axial slice locations. A and B depict the same axial cross section with the conventional cardiac reconstruction shown in A compared to the DL-based image de-blurring method shown in B. C and D show a lower axial slice. Again, conventional processing in C is compared to the processing with DL image de-blurring active as shown in D.

Conclusions

- We investigated the impact of a generic DL image de-blurring algorithm on **CAC detection** and perceived **image sharpness**, showing improvements, both quantitatively for the chest phantom as well as qualitatively on the clinical cardiac scans.
- Further, we want to promote this intricate interplay between **denoising** and **de-blurring** with AI algorithms, where we herein introduce a quite generic AI de-blurring algorithm trained on **natural images**.
- Last, we want to promote the use of **clinical task-based metrics** to assess **image formation** algorithms such as the CAC detection task.

References

- Greffier, J. et al., *Med Phys.* **49(8)**, 5052-5063, 2022
- Lee, T.-C., et al., *Proc. SPIE* 12304, 2022
- Groen, J. M. et al., *Eur. J. Radiol.* **82(2)**, e58-e68, 2013
- van der Werf, N. R. et al., *Eur. Radiol.*, **32(1)**, 152-162, 2022
- Yuan, Y. et al., *Med. Img.: Physics of Med. Img.*, SPIE 124634, 2023
- Wülker, C. et al., *Proc. Fully3D*, 2023
- Zabic, S. et al., *Med. Phys.*, **40(3)**, 031102, 2013
- Mohan, S. et al., *arXiv:1906.05478*, 2020
- Kingma, D. P. and Ba, J., *arXiv:1906.05478*, 2020
- Agustsson, E. and Timofte, R. et al., *IEEE CVPRW*, 1122-1131, 2017
- van Praagh, G. D., et al., *Med. Phys.*, **48(7)**, 3730-3740, 2021